Design of a Humanoid Biped Robot for Walking Research

Daniel Paluska, Jerry Pratt, David Robinson, Gill Pratt

MIT Leg Laboratory
Cambridge, MA 02139
http://www.ai.mit.edu/projects/leglab/robots/m2/m2.html

Abstract. A humanoid bipedal robot(M2) was developed at the MIT Leg Laboratory. The goal of the robot is to provide a robust platform for walking research. We surveyed existing data of humans and performed numerous simulations in order to determine the design specifications. We kept passive dynamics in mind and tried to stay close to mechanical characteristics we believe simplify walking control. Degrees of freedom above the waist are absent because we wanted the minimum complexity possible for walking. The resulting robot has 12 active degrees of freedom. All the active degrees of freedom are powered using Series Elastic Actuators, which provide force control and shock tolerance. The robot weight is approximately 28kg(62lbs) and the hip height is 0.97m(37in). Currently the robot is standing and balancing on its own.

1 Introduction

We recently built a new bipedal robot in the Leg Laboratory. A picture of the assembled biped is shown in Figure 1. The robot is humanoid in degrees of freedom and link sizes below the waist. It is without any degrees of freedom above the waist. The approximate weight of the robot is 28kg(62lb) and it's hip height is roughly 0.97m(37in). In this paper we will discuss the robot's specifications and present some human and simulation data which lead us to those specifications.

The main goal of the robot is to act as a robust platform for bipedal walking research. Other goals include walking 1 m/s, climbing normal stairs, looking biological, turning dynamically, a three year life and ten hours working time between failures. There are four main areas where our efforts were concentrated.

1. **Series Elastic Actuators** Series Elastic Actuators[10] are used for all of the active degrees of freedom. These actuators provide force control as well as shock tolerance. We believe both are an absolute necessity for the task of biologically similar walking. The low output impedance of the actuators allows us to take advantage of the robot's natural dynamics. All joints employ the same actuator design to minimize complexity and facilitate repairs.
2. **Human Proportions** The use of human sizing allows for easy comparison with biomechanics data and intuition. Human sizing also allows for use of

large, standard components which are easy to see and debug. The research stays focused on walking and not miniaturization.

3. **Lightweight** The robot frame is carbon fiber and most remaining components are plastic or aluminum. The necessary actuator forces are kept low. Less mass makes the robot more manageable in a research environment. It is easier to handle and less likely to damage itself or harm researchers.

4. **Mechanical Control Mechanisms** Each joint(most importantly the knee) has adjustable stops with rubber pads. The foot of the robot is equipped with a passive toe joint. This joint has an adjustable range as well as a return spring. The limit stops are essentially high frequency non-linear PD loops which are difficult to implement in digital control even with the use of sophisticated electronics and sensors. The low impedance actuators are also allow for uncertain contact, a necessity for walking on rough terrain. These mechanical features eliminate the need to operate any high frequency control loops on the robot.
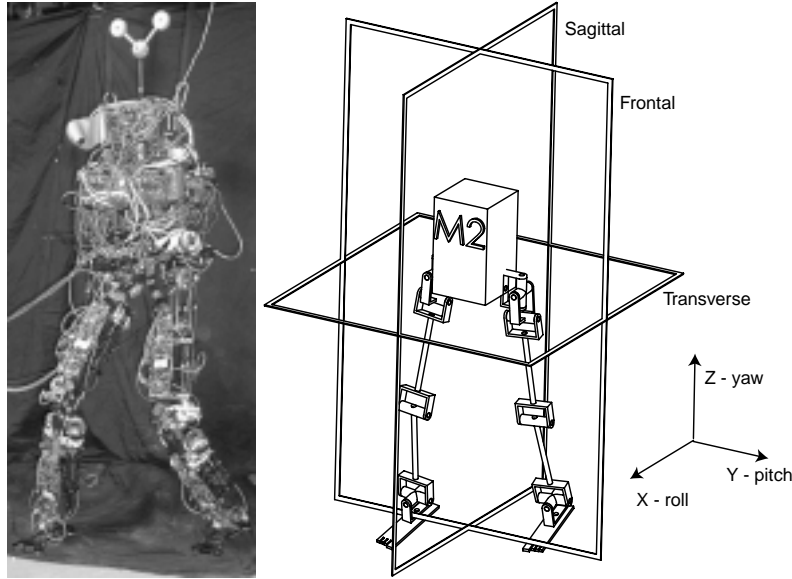
Fig. 1. A photo of the completed robot and a joint schematic view of the robot. The schematic shows active degrees of freedom only. The optional passive toe joint is not shown.

The robot is a three-dimensional continuation of the work that began with Spring Turkey[5] and continued with Spring Flamingo[6]. The above points are the key areas where it differs from some other three dimensional walkers[8, 7] which employ high impedance actuation and trajectory following control schemes.

2   The Design

2.1   Overall Structure

A photo of the robot and a joint schematic view are shown in Figure 1. The leg of the robot has six active degrees of freedom plus an optional passive degree of freedom in the foot. The vertical axis, Z, is the yaw axis. The X axis is the roll axis and the Y axis is the pitch axis. The hip has three degrees of freedom. These three degrees of freedom are made up of a universal joint (yaw and roll) followed by a pin joint (pitch). The pin joint is offset slightly(2cm).
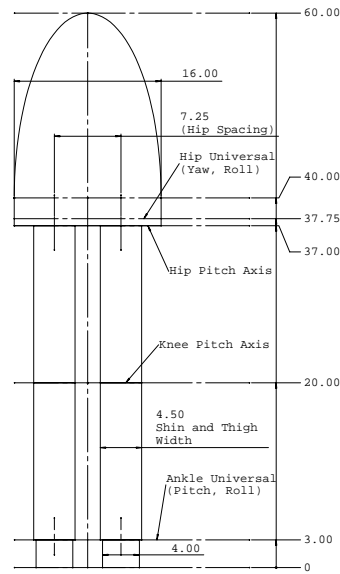
Fig. 2. The dimensions of the biped in the frontal plane. The body and links are approximately axially symmetric about their longitudinal axis. Dimensions are in inches.

The frontal plane dimensions of the robot are shown in Figure 2. The dimensions are very close to the dimensions for a 50th percentile US male as given by Whitney[2]. The ranges of motion are adapted from robot simulations and data found in Rose, et al.[15] , Winter[14] and Kapandji[9].

The mass distribution of the robot is dominated by the location of the actuators within the links. As a result, the robot's mass distribution is centered lower than an average human's. Table 2.1 shows the percentage mass distributions for an average male, the Leg Lab robot and a planar passive dynamic walker[12]. The robot mass distribution is closer to that of a planar passive dynamic walker than a human. However, due to successful computer simulations[3], we did not believe it would be worthwhile to add additional weight to the torso in order to put the proportions more in line with a human.

	deg	rad/s	Nm	Drive Type
hip(pitch)	80,-30	7.3333	50	Pulley
hip(roll)	30,-20	6.8	59	Push-rod
hip(yaw)	30,-15	5.5	67	Push-rod
knee(pitch)	80,0	8.8	42	Push-rod
ankle(pitch)	45,-20	8.8	88*	Push-rod
ankle(roll)	20,-20	7.3	100*	Push-rod

Table 1. Robot Joint Specifications. Torque and rad/s numbers are given for maximum moment arm. Power, torque and velocity are symmetric due to the actuator. *The ankle roll and pitch are not independent. Their maximum values can not be applied simultaneously.

	deg	rad/s	Nm	W
hip(pitch)	30,-18	3.6,-2.0	-111.0	56
hip(roll)	8,-7	1.6,-1.0	-63.5	+-28
hip(yaw)	5,-15	4.0,-3.0	8.0	-16
knee(pitch)	68,8	5.8,-7.8	-71.4	-79.5
ankle(pitch)	10,-15	3.0,-4.2	-63.5	280
ankle(roll)	na	NA	40.0	-16

Table 2. Human walking parameters from normalized data contained in *Human Walking.* Forces and power calculated for a for 1.83 m(6'2"), 80 kg(178lb) person. Table displays non-concurrent maximum values which occur during an average walking cycle.

Body Part/Area	Human	Biped Robot	PDW
Shin & Foot (x2)	6%	13.5%	10%
Thigh (x2)	10%	11%	15%
Ab/Pelvic	27%	51 %	50%
Arm (x2)	5%	NA	NA
Thorax to Head	31%	NA	NA

Table 3. Approximate distribution of mass in humans, the Leg Lab biped M2 robot and in McGeer's kneed passive dynamic walker(PDW). Human data adapted from Dempster and Gaughran [16]. Robot weight distribution is driven primarily by actuator locations. Each actuator is approximately 1.1kg(2.5 lbs).

2.2   Actuators

The actuators used in the robot are 90W, 1.2KG Series Elastic Actuators[1]. They are capable of a maximum force of roughly 1320N (300lbs) and a maximum speed of roughly 0.28 m/s (11 in/s). The actuators have a force control bandwidth of 30Hz. Linear actuators where chosen over rotary actuators due to the available space in the robot. Linear actuators allowed for placement along the longitudinal axis of the leg links. The actuators are symmetric in their power, speed and force capabilities.

2.3   Ankle

The ankle of the biped is a universal joint. Pitch is followed by roll. This is a slight deviation from the structure of the human ankle. The human ankle is often likened to a universal joint where the second axis is at 45 degrees to the first rather than at 90 degrees[9]. For engineering simplicity we use a universal joint with orthogonal axes. The instantaneous power requirement for ankle pitch is the greatest. The actuators were placed in a configuration so they can act together in the pitch direction.

A prototype of the ankle is shown in Figure 3 and a schematic of the ankle and its actuators are shown in Figure 4. The ankle has two series elastic actuators placed along the longitudinal axis of the shin. The actuators are mounted by a universal joint near the top of the shin and attached to the foot by a ball and socket joint (rod-end). This is a linkage variation of a standard geared differential. When the actuators push in unison, a moment is generated about the pitch axis. When they push in opposite directions, a roll moment is generated.

2.4   Foot

Two different feet were designed for the robot. One foot is a simple rectangular design with four single axis load cells residing at each of the corners. This foot closely resembles the foot that was used in computer simulations in the lab. Another more involved foot was designed in order to explore the roll of the toes in walking.

The second foot of the biped robot contains a passive joint which is modeled after the toe of a human. The joint is believed to smooth the center of mass trajectory of the body during a walking cycle[15]. The toe joint is simply a pin joint with two limit stops and a soft return spring.

Ground contact and sensing on the foot consists of four single axis load cells. One cell is placed at the heel, and three cells are placed in a triangle at the toe/ball of the foot. The three cells in the toe are all constrained to the same plane. The three toe contact points can rotate about the foot Y-axis with respect to the heel contact point. The layout of the sensors can be seen in Figure 5.

Standard through-hole button load cells are used. There is a rubber bumper roughly 0.875" in diameter attached to each load cell which contacts the ground. On the simple four point foot there is a rectangular pastic piece with a 0.25"
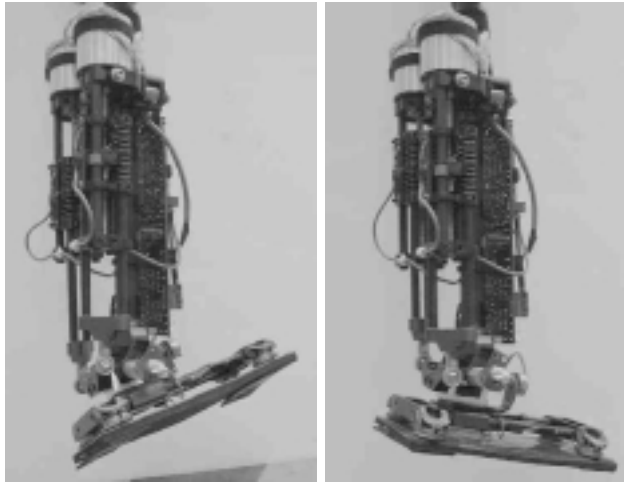
Fig. 3. The robot lower leg. The ankle is shown in two different positions. Two actuators control the roll and pitch of the foot with respect to the shin. Two analog potentiometers measure the angle of the foot with respect to the shin. An analog PCB supplies power to the actuator and joint potentiometers and sends and receives data from the DSP.

piece of neoprene for grip and shock absorbtion. This can be seen in Figure 3. Single axis load cells were chosen over a six axis sensor because of their size and weight, and chosen over strain gauges because of their ease of use and quick replaceablility.

On the more complicated biped foot, force control and a passive toe joint are the reasons the four contact points of the foot are not over-constrained. Since ankle roll is force controlled rather than position controlled, it can adjust itself so the three points of the toe lie flat. Then the passive toe joint(a pitch joint) allows the fourth point on the heel to lie flat as well.

2.5 Hip

The biped hip has three degrees of freedom. The joint consists of a universal joint followed by a slightly offset pin joint. A schematic of the hip is shown in Figure 6. The yaw axis is first and the the yaw actuator is mounted to the body frame with a pin joint. The roll actuator is next. Since its attachment point passes through the roll angle, it is mounted to the body by a universal joint. Its endpoint is attached by a ball and socket joint. The pitch actuator, which is not shown, lies along the longitudinal axis of the thigh. It is the only actuator which is attached using a cable and pulley rather than a rod-end. The range of motion of the hip pitch joint is the largest. The moment arm changes associated with a drive arm would be too great at the extents of the motion. At sixty degrees from the perpendicular drive position, the moment arm would be half its original length.
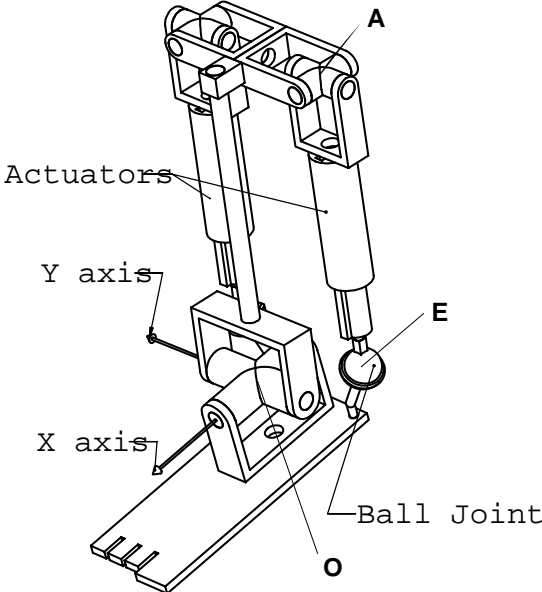
Fig. 4. A schematic of the ankle joint actuation scheme. The axes shown are fixed to the center of the universal joint. The points A,E, and O are referenced in Section 3.
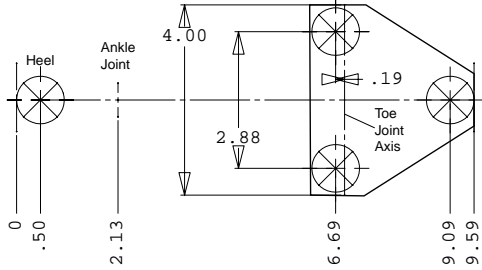
Fig. 5. The dimensions of the biped foot. The X's represent the location of the load cells.
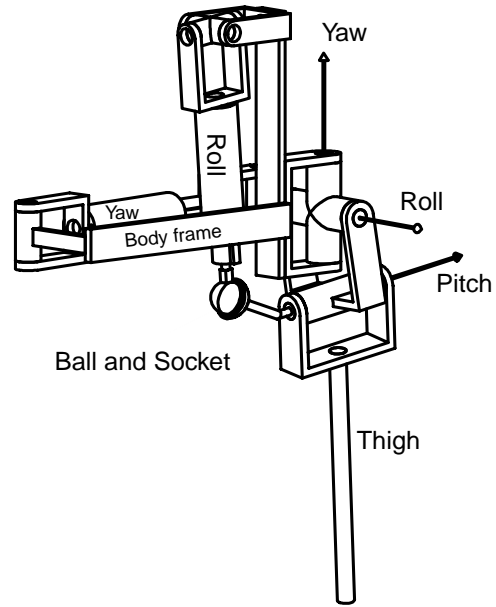
Fig. 6. A schematic of the biped hip. The pitch actuator is not shown. It lies along the axis of the thigh.
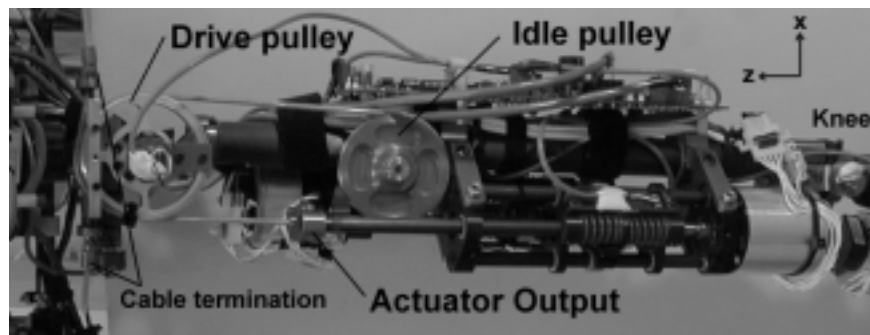
Fig. 7. A photo of the biped thigh illustrating the hip pitch cable drive system.

3   Electronics and Control

The basic electronic subsystems of the robot are shown in Figure 8. The robot is powered by a 48 Volt power supply. There is also an Ethernet connection not shown in the figure which can be used to load control code and retrieve data from the on-board computer.

There are twelve actuators and motor amplifiers. There are six two channel analog force control and joint potentiometer buffer circuit boards. The actuator controllers and joint potentiometer buffers are local to the actuators and joints. There is one in each shin, one in each thigh and two in the body. They are PCB's which where designed in the Leg Lab. All signals are sent and received differentially between the computer and the analog boards. There are four instrumentation boards for the load cells in the feet. These boards are located in the shins. In the body there is a power supply board which transforms the 48V to +/-5 and +/-12 for the computer, vestibular system and instrumentation amps. The analog PID boards and the brushless motor amplifiers run on 48V.
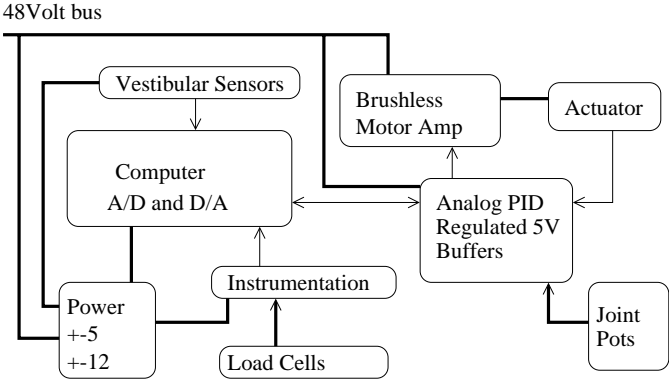
Fig. 8. An overview of the biped electronics. Thick lines indicate power transfer and arrowheads indicate information flow.

The control code runs on the computer(TI C-31 based dsp) and sends desired forces to the analog boards. The analog boards have PD control loops for the Series Elastic Actuators. This is essentially the same method used for Spring Flamingo. The main differences are the addition of Ethernet for faster communication with the outside world and differential send and receive for signals within the robot. The differential amplifiers and recievers minimize succeptibility to noise.

4   Joint Actuator Force and Torque Transformations

All the joints of the robot are rotary joints and they are powered by linear actuators. A little math is required to transform a desired torque at the joint, τ, into a desired force, F, at the actuator.

The hip pitch is the simplest of all because it is a cable drive and $F = \frac{\tau}{r}$ holds throughout the range of motion. The rest of the joints require a more complicated equation because the angle between the moment arm and the actuator changes with the joint angle. We will consider the knee in detail and the other joints are simple extensions of the knee math and described fully in Paluska[4].

The knee actuator is connected to the knee joint via a push rod of length $|O_k A_k| = r_k$ at the shin and fixed a pin joint at the thigh.

The knee joint has three point of interest which we will use for the derivation of the transformation. The knee pivot O_k, the actuator pushrod attachment A_k and the actuator mounting pivot M_k. The robot knee joint and points can be seen in Figure 9 and a simple line drawing is seen in Figure 10.

$$\tau = r \times F = r_k \sin(\angle O_k A_k M_k) F_{act} \tag{1}$$

The actuator force required given tau_k is

$$F_{knee} = \frac{\tau_k}{r_k \sin(\angle O_k A_k M_k)} \tag{2}$$

where $\angle O_k A_k M_k$ can be defined as follows

$$\angle O_k A_k M_k = \theta_{fixed} + \theta_k - \angle A_k M_k = \theta_{fixed} + \theta_k - \arctan \frac{r \sin(\theta_{fixed} + \theta_k) - L_2}{L_1 + r \sin(\theta_{fixed} + \theta_k)} \tag{3}$$

The angle between the shin and the thigh is θ_k and the constant θ_{fixed} is the angle between shin and the segment $O_k A_k$. It is also possible to derive the equations avoiding the inverse tangent by using the law of cosines.
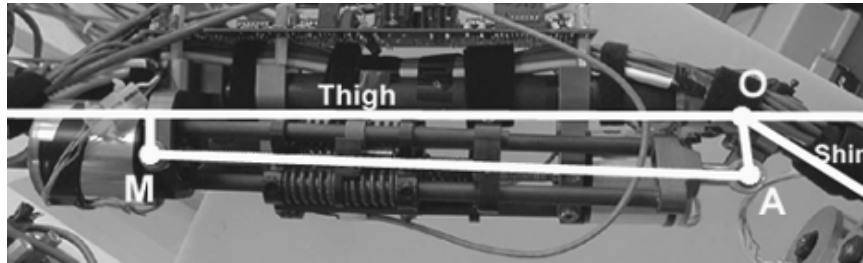
Fig. 9. A photo of the robot knee joint with superimposed lines and points. Points O, A and M all refer to pin joints. O is the knee joint. M is where the actuator is mounted to the thigh and A is where the actuator is attached to the shin. this view is the opposite side of the thigh as shown in Figure 7.
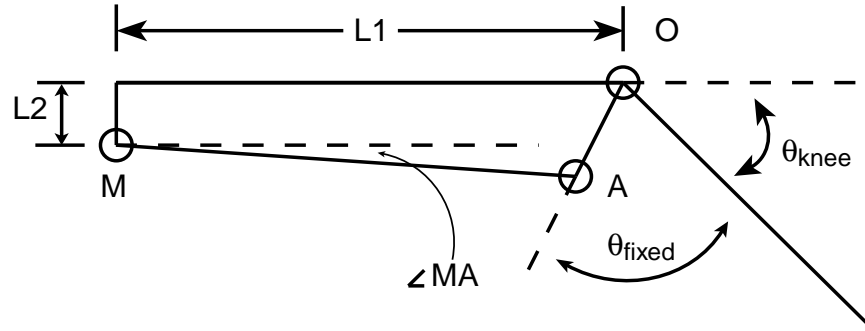
Fig. 10. A line drawing of the knee for the calculation of knee actuator desired force. The actuator is the line segment MA. This drawing also pertains to the geometry of the hip and ankle joints but the hip and ankle actuators have motions out of the plane whereas the knee actuator is always in the plane perpendicular to the knee axis.

Component	QTY	Each US $	Total US $
Actuator, Amp	12	1500	18,000
Custom Computer	1	10,000	10,000
CFRP frame	8	300	2500
Machining	1	30,000	30,000
Vestibular	1	10,000	10,000
Misc Parts	200	20	4000
PCB's	10	1,000	10,000
Load Cells	8	450	3600
TOTALS			88,100

Table 4. Basic robot budget. See Robinson et al.([1]) for more detail on the actuator. This budget does not include prototyping or development costs. Part quantities and individual costs are not necessarily meant to imply identical parts but rather to give an average price for all units of a certain type.

5   Summary

The robot construction was completed in April 2000. Currently the robot can balance unsupported during standing and knee bends. Development and debugging of the walking control algorithm is in progress. The robot had been in development since summer of 1998. The basic cost of parts is shown in Table 4. This table does not include development or prototyping costs. Also, certain items, such as CFRP, vary widely in cost for different areas so the *Each* column is simply the average cost rather than the exact cost. Further details of the robot design, parts, costs, and schedule can be found on the Leg Lab web site.

Acknowledgments

References

1. D.W. Robinson, J.E. Pratt, D.J. Paluska, and G.A. Pratt. Series Elastic Actuator Development for a Biomimetic Walking Robot. *IEEE/ASME AIM99*, Sept 20-23, 1999. Atlanta, GA.
2. Henry Dreyfus Associates. *The Measure of Man and Woman.* Whitney Library of Design. New York. 1993.
3. J.E. Pratt, and G.A. Pratt. Exploiting Natural Dynamics in the Control of a 3D Bipedal Walking Simulation. *to be presented in CLAWAR*, Sept, 1999. Portsmouth,UK.
4. D. J. Paluska. Design of a Humanoid Biped Robot for Walking Research. *Masters Thesis, MIT*, Sept, 2000.
5. J.E. Pratt, P. Dilworth and G.A. Pratt. Virtual model control of a bipedal walking robot. *IEEE Conference on Robotics and Automation*, pages 193-198, 1997.
6. J.E. Pratt, and G.A. Pratt. Exploiting Natural Dynamics in the Control of a Planar Bipedal Walking Robot. *Proceedings of the thirty-Sixth Annual Allerton Conference on Communication, Control, and Computing*, pages 739-748, 1998.
7. J. Yamaguchi, S. Inoue, D. Nishino, and A. Takanishi Development of a bipedal humanoid robot having antagonistic driven joints and three dof trunk. *IEEE Conference on Intelligent Robotics and Systems*, 1998.
8. K. Hirai, M. Hirose, Y. Haikawa, and T. Takenaka. The Development of the Honda Humanoid Robot. *IEEE Conference on Robotics and Automation*, 1998.
9. I. A. Kapandji. *Physiology of the Joints, Volume Two, Lower Limb.* Churchill Livingstone. 1998.
10. G. A. Pratt and M. Williamson. Series Elastic Actuators. *IEEE International Conference on Intelligent Robots and Systems*, pp. 399-406, 1995.
11. T. McGeer. Passive Dynamic Walking. *International Journal of Robotics Research*, vol. 9, no. 2, pp. 62-82, 1990.
12. T. McGeer. Passive Dynamic Walking Catalogue. *Experimental Robotics*, 1991.
13. M. Garcia, A. Chatterjee, and A. Ruina Stability and control of passive locomotion in 3d. *International Conference on Robotics and Automation*, pp. 2351-2356, 1998.

14. D. A. Winter. *Biomechanics and Motor Control of Human Movement.* John Wiley and Sons, Inc. New York. 1990.

15. J. Rose and J. G. Gamble, eds. *Human Walking.* Lippincott, Williams and Wilkins. 1996.

16. W. T. Dempster and G. Gaughran. Properties of Body Segments Based on Size and Weight. *American Journal of Anatomy.* 1965.